DOI: 10.1534/genetics.109.102327

p53-Independent Apoptosis Limits DNA Damage-Induced Aneuploidy

Laura M. McNamee and Michael H. Brodsky[1]

Program in Gene Function and Expression and Program in Molecular Medicine, University of Massachusetts Medical School, Worcester, Massachusetts 01605

Manuscript received February 28, 2009
Accepted for publication March 18, 2009

ABSTRACT

DNA damage or unprotected telomeres can trigger apoptosis via signaling pathways that directly sense abnormal DNA structures and activate the p53 transcription factor. We describe a p53-independent mechanism that acts in parallel to the canonical DNA damage response pathway in Drosophila to induce apoptosis after exposure to ionizing radiation. Following recovery from damage-induced cell cycle arrest, *p53* mutant cells activate the JNK pathway and expression of the pro-apoptotic gene *hid*. Mutations in *grp*, a cell cycle checkpoint gene, and *puc*, a negative regulator of the JNK pathway, sensitize *p53* mutant cells to ionizing radiation (IR)-induced apoptosis. Induction of chromosome aberrations by DNA damage generates cells with segmental aneuploidy and heterozygous for mutations in ribosomal protein genes. p53-independent apoptosis limits the formation of these aneuploid cells following DNA damage. We propose that reduced copy number of haploinsufficient genes following chromosome damage activates apoptosis and helps maintain genomic integrity.

EUKARYOTIC cells employ diverse mechanisms to preserve the structure and function of their genome following chromosome damage. Unicellular organisms rely on DNA repair systems and cell cycle arrest to prevent propagation of genome damage, while multicellular organisms can also activate programmed cell death pathways to eliminate cells following damage (Sancar *et al.* 2004; Roos and Kaina 2006; Bartek and Lukas 2007; Harper and Elledge 2007). In response to double-strand DNA breaks (DSBs), the Mre11, Rad50, and Nbs1 (MRN) complex helps process the damage and activates the ATM and ATR kinases. ATM and ATR phosphorylate many substrates including the downstream kinases Chk1 and Chk2, which regulate cell cycle arrest and apoptosis. The p53 transcription factor plays an evolutionarily conserved role, connecting the DNA damage signaling pathway to the core apoptotic machinery (Murray-Zmijewski *et al.* 2006; Helton and Chen 2007). Mammalian p53 is directly phosphorylated by ATM and Chk2 and activates many targets genes including pro-apoptotic Bcl-2 family members and the cell cycle regulator p21 (Riley *et al.* 2008). The p53 paralogs p63 and p73 also contribute to p53-dependent apoptosis by helping p53 bind the promoters of pro-apoptotic genes in some, but not all cell types (Flores *et al.* 2002; Senoo *et al.* 2004).

Supporting information is available online at http://www.genetics.org/cgi/content/full/genetics.109.102327/DC1.

[1]*Corresponding author:* 623 Lazare Research Bldg., Program in Gene Function and Expression, University of Massachusetts Medical School, 364 Plantation St., Worcester, MA 01605.
E-mail: michael.brodsky@umassmed.edu

While p53 is required for normal induction of cell death following DNA damage, p53-independent mechanisms can also activate a reduced or delayed response (Yuan *et al.* 1999; Irwin *et al.* 2003; Urist *et al.* 2004; Ozaki and Nakagawara 2005; reviewed in Roos and Kaina 2006). Several studies have demonstrated that p53-independent death can be enhanced by inactivating checkpoints that block cell cycle progression in the presence of unrepaired DNA damage. In one example, cancer cells lacking p53 required ATM, ATR, Chk1, and p38MAPK/MK2 signaling for cell cycle arrest; loss of this response led to caspase-3 activation and mitotic catastrophe following DNA damage (Reinhardt *et al.* 2007). In another case, zebrafish embryos lacking p53 and Chk1 function required ATM and ATR to activate an unusual apoptotic response requiring caspase-2, but not caspase-9 or caspase-3 (Sidi *et al.* 2008).

In Drosophila, rapid induction of apoptosis by ionizing radiation (IR) or unprotected telomeres requires homologs of ATM, Chk2 (TEFU, MNK, respectively), and p53 (Brodsky *et al.* 2000a, 2004; Ollmann *et al.* 2000; Xu *et al.* 2001; Peters *et al.* 2002; Oikemus *et al.* 2004; Silva *et al.* 2004; Song *et al.* 2004). G_2 arrest requires ATR, ATRIP, and Chk1 (MEI-41, MUS304, and GRP, respectively) (Hari *et al.* 1995; Fogarty *et al.* 1997; Brodsky *et al.* 2000b, 2004; De Vries *et al.* 2005). Transcriptional targets of p53 include the pro-apoptotic genes *reaper* (*rpr*), *head involution defective* (*hid*), and *sickle* (*skl*) (Brodsky *et al.* 2000a, 2004; Christich *et al.* 2002; Akdemir *et al.* 2007). *hid* is essential for the rapid induction of apoptosis, while *rpr* may play a less significant role (Brodsky *et al.* 2004; Moon *et al.* 2008). *rpr*, *hid*, and

skl encode proteins that induce apoptosis by directly binding and inhibiting DIAP1, leading to activation of an initiator caspase, Dronc, and effector caspases (Bergmann *et al.* 2003; Chew *et al.* 2004; Daish *et al.* 2004; Waldhuber *et al.* 2005; Kondo *et al.* 2006; Xu *et al.* 2006; Steller 2008). Regulation of mitochondrial ultrastructure by HID and RPR may also help induce cell death after DNA damage (Holley *et al.* 2002; Olson *et al.* 2003; Abdelwahid *et al.* 2007; Goyal *et al.* 2007).

While rapid induction of apoptosis following IR requires Drosophila p53, there is also p53-independent apoptosis following chromosome damage. Mutations in the Drosophila ATM/ATR/MRN damage signaling pathways lead to loss of telomere protection and high levels of spontaneous apoptosis (Bi *et al.* 2004, 2005; Ciapponi *et al.* 2004, 2006; Oikemus *et al.* 2004, 2006). The apoptosis induced by unprotected telomeres is only partly suppressed by loss of p53 or MNK (Oikemus *et al.* 2004, 2006). No additional p53 family members contribute to this response since Drosophila has only a single p53 homolog. Similarly, in the absence of p53, a delayed or reduced induction of apoptosis is observed following IR or telomere loss (Wichmann *et al.* 2006; Titen and Golic 2008). Double-mutant combinations of *tefu*, *mus304*, and *nbs* also exhibit spontaneous apoptosis, suggesting that the activation of apoptosis by chromosome damage is independent of the central upstream components of the DNA damage response pathway (Oikemus *et al.* 2006).

Here, we characterize the regulation and function of p53-independent apoptosis following IR. We show that p53-independent apoptosis requires *hid*, which is a target of IR-induced JNK signaling. Mutations in *grp* or the JNK phosphatase *puc* sensitize *p53* mutant cells to IR-induced apoptosis, suggesting that cell cycle progression and JNK signaling are critical for this response. We find that this response acts to maintain genomic stability by reducing the number of aneuploid adult cells induced by IR. We propose that activation of JNK and HID in response to aneuploidy induces p53-independent apoptosis following IR.

MATERIALS AND METHODS

***Drosophila melanogaster* genetics:** All flies were raised at 25°. Genes and alleles are described in http://flybase.org. w^{1118} was used as the wild-type strain. The following mutant genotypes were used: $p53^{11\text{-}1b\text{-}1}$ (this allele is used for all experiments except in Figure S3B); $p53^{5A\text{-}1\text{-}4}$; mnk^{P6}; grp^{fs1}; $p53^{11\text{-}1b\text{-}1}$; grp^{fs1} mnk^{P6}; *actin-Gal4/+; UASp35/+*; *en-Gal4/+; UASp35/+*; *en-Gal4/+; UASp35* $p53^{11\text{-}1b\text{-}1}/p53^{11\text{-}1b\text{-}1}$; *en-Gal4/+;UASpuc* $p53^{11\text{-}1b\text{-}1}/p53^{11\text{-}1b\text{-}1}$; *en-Gal4/+; UASpuc UASp35* $p53^{11\text{-}1b\text{-}1}/p53^{11\text{-}1b\text{-}1}$; *en-Gal4/+; puc*^{A29}*lacZ* $p53^{11\text{-}1b\text{-}11}$*/+ UASp35* $p53^{11\text{-}1b\text{-}1}$; *puc*^{A29}*-lacZ* $p53^{11\text{-}1b\text{-}1}/+p53^{11\text{-}1b\text{-}1}$; grp^{fs1}; *puc*^{A29}*-lacZ* $p53^{11\text{-}1b\text{-}1}/+p53^{11\text{-}1b\text{-}1}$; $brk^{38\text{-}20}$*-lacZ/+; p53*$^{11\text{-}1b\text{-}1}$; $brk^{38\text{-}20}$*-lacZ/+; en-Gal4/+;UASp35* $p53^{11\text{-}1b\text{-}1}/p53^{11\text{-}1b\text{-}1}$; $brk^{38\text{-}20}$*-lacZ/+; en-Gal4/+;UASp35/+*; *dronc*^{I29}*/dronc*^{I24}; hid^{X14}/hid^{05014}; hid^{X14} $p53^{11\text{-}1b\text{-}1}/$ hid^{05014} $p53^{11\text{-}1b\text{-}1}$; mwh^1; and mwh^1 $p53^{11\text{-}1b\text{-}1}$.

Analysis of X-irradiation-induced changes in apoptosis, cell cycle, and gene expression: For 4- and 8-hr time points, wandering third instar larvae were mock treated or X-irradiated with 4000 rad using a Faxitron RX650 X-ray cabinet system (Faxitron X-ray Corporation). For 12-, 16-, and 24-hr time points, larvae were treated as early third instar in Drosophila media and dissected as wandering third instar larvae.

Immunostaining and acridine orange staining were largely performed as described previously (Abrams *et al.* 1993; Brodsky *et al.* 2000b; Oikemus *et al.* 2004). Imaginal wing discs from wandering third instar larvae were dissected in 1× PBS and fixed in 4% formaldehyde for 30 min at room temperature. Samples were washed in 250 μl of PBS + 0.3% Triton X-100 five times for 5 min each and incubated in blocking solution (PBS + 0.3% Triton X-100 + 5% normal goat serum) for 1 hr. Samples were incubated in primary antibody diluted in blocking solution overnight at 4°. The posterior expression domain in *en*-Gal4 experiments was marked by expression of endogenous En protein. Primary antibodies were used at the following dilutions: rabbit anti-cleaved caspase-3 (Cell Signaling Technology), 1:100; mouse anti-phospho-H3 (Cell Signaling Technology), 1:500; mouse anti-Beta-Gal (Santa Cruz Biotechnology), 1:1000; mouse anti-EN (Developmental Studies Hybridoma Bank at the University of Iowa, DSHB), 1:10; mouse anti-WG (DSHB), 1:50; mouse anti-PTC (DSHB), 1:100; and guinea pig anti-HID (Ryoo *et al.* 2004) (gift from Hyung Don Ryoo, New York University Medical Center), 1:500. Following primary antibody incubation, samples were washed five times for 5 min each and incubated with secondary antibody in blocking solution for 2 hr at room temperature. Secondary antibodies were used at the following dilutions: anti-mouse Alexa 488 (Molecular Probes, Eugene, OR), 1:2000; anti-rabbit Alexa 555 (Molecular Probes), 1:2000; anti-guinea pig Alexa 488 (Molecular Probes), 1:2000; anti-mouse FITC (Jackson Laboratories, for staining with anti-phospho-histone H3 primary), 1:250; and anti-mouse Cy5 (Jackson Laboratories), 1:250. Imaginal wing discs were stained with 4′,6-diamidino-2-phenylindole (DAPI) and mounted in Vectashield (Vector Laboratories, Burlingame, CA). Wide field images of wing discs were acquired with a Zeiss Axioplan fluorescence microscope, an ORCA-ER digital camera (Hamamatsu), and Axiovision 4.5 software. Confocal images were acquired with a Leica TCS SP2 confocal microscope. At least five wing discs were scored for each genotype and time point.

Quantitative analysis of cleaved-caspase staining: A confocal *z*-series was taken through the entire disc at intervals of 1.42 μm with a 20× objective. A three-dimensional reconstruction was generated using Imaris image analysis software (version 5.0.1, Bitplane). A high-intensity threshold was used to create isosurfaces of regions that stained positive for cleaved caspase-3. A low-intensity threshold was used to create an isosurface of the background staining observed throughout the entire disc. Examples of a maximum-intensity projection, low-threshold isosurface, and high-threshold isosurface are shown in Figure 1E. The anti-caspase-3 index is the total volume of high-intensity isosurfaces divided by the volume of the low-intensity isosurface. *P*-values were calculated with a two-tailed Student's *t*-test.

***Minute* assay:** Newly laid eggs were collected for 48 hr. Seven days later, larvae were X-irradiated with 0, 500, 1000, or 2000 rad at two different stages, either wandering late third instar or second to early third instar larvae still in the media. Late third instar larvae were transferred to new vials following IR. For larvae irradiated in the media, wandering third instar larvae were picked out of the vials over the next 48 hr. After 1 week, the numbers of normal and *Minute* bristles were scored in the resulting adults as previously described (Brodsky *et al.* 2000b). For each genotype and treatment, bristle phenotypes were scored in at least 60 flies unless otherwise noted. Data

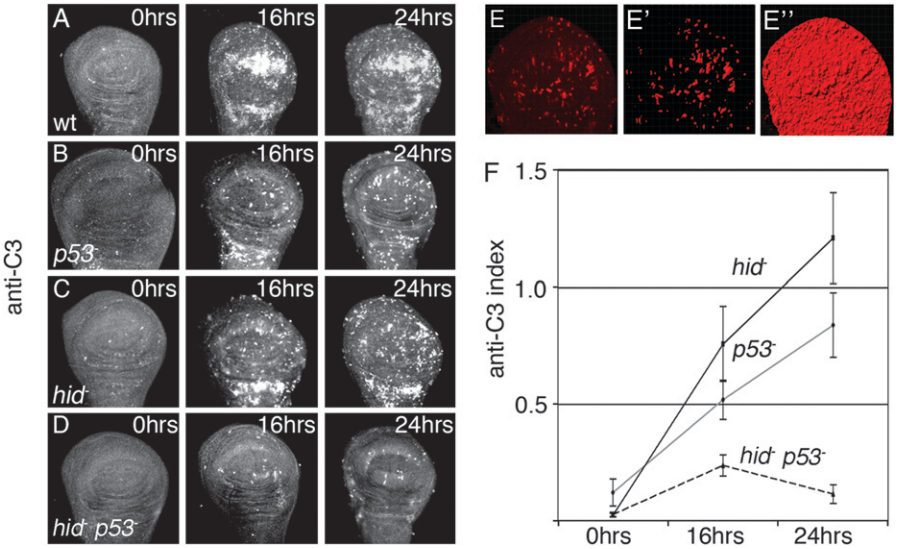

FIGURE 1.—*hid* regulates p53-independent apoptosis. (A–D) Apoptosis was assayed in wild-type (wt), *p53*, and *hid* single-mutant and *p53 hid* double-mutant imaginal wing discs at different time points following ionizing radiation (IR) by staining with an antibody to cleaved caspase 3 (anti-C3). (A) Induction of apoptosis is observed from 4 to 16 hr following DNA damage in wt wing discs. (B–D) Apoptosis is delayed and reduced in *p53* and *hid* single-mutant wing discs compared to wild type. Apoptosis is not induced in *p53 hid* double-mutant wing discs at 16 and 24 hr following IR. (E–E″) Quantification of anti-C3 staining (see MATERIALS AND METHODS). (E) A maximum-intensity projection of a confocal *z*-series obtained from an imaginal wing disc stained with anti-C3. (E′) A high-intensity threshold was used to create an isosurface for anti-C3-stained regions. (E″) A low-intensity threshold was used to create an isosurface for the entire disc. (F) The volume of anti-C3-positive tissue divided by total disc volume is expressed as a percentage at 0, 16, and 24 hr after treatment with IR. Anti-C3 staining does not increase in *hid p53* double-mutant discs and is significantly lower than observed for *p53* single-mutant discs (*P*-value <0.01). For all discs and data points shown, at least five discs were analyzed. Error bars indicate the standard error of the mean.

from three different irradiation experiments were pooled. *P*-values were calculated with a two-tailed Student's *t*-test.

***mwh* assay:** Wandering third instar larvae were irradiated with 0, 250, or 1000 rad and transferred to new vials. After 1 week, adult wings were mounted in 1:1 methyl salicylate/Canada balsam (Sigma, St. Louis) and individual cells were scored for the $mwh^{-/-}$ phenotype (BRODSKY *et al.* 2000b). For each genotype and dose, five wings were scored. *P*-values were calculated using a two-tailed Student's *t*-test.

RESULTS

p53-independent apoptosis requires the pro-apoptotic gene *hid* and the apical caspase gene *dronc*: Cell death in Drosophila wing discs was examined following X-irradiation of third instar larvae. At least five discs were examined for every genotype and time point shown. Mutant alleles are described in MATERIALS AND METHODS. Four hours after irradiation, high levels of apoptosis are induced in wild-type discs (Figure 1A; Figure S1A and Figure S2A). *p53* or *mnk* mutant discs exhibit no change at 4 hr, but a significant increase in apoptosis between 16 and 24 hr (Figure 1, B and F; Figure S2, B and C). A previous study indicated that one or more of the pro-apoptotic genes in the *Df(3L)H99* region are likely to contribute to p53-independent apoptosis following IR (WICHMANN *et al.* 2006). In *hid* single-mutant discs, apoptosis is blocked at 4–8 hr following IR and is reduced at later time points (Figure 1, A and C; Figure S2, A and F). Twenty-four hours following IR, *hid, p53* double-mutant discs exhibit a 7- and an 11-fold reduction in the caspase staining compared to *p53* or *hid* single-mutant discs (Figure 1, B–F), demonstrating that *hid* contributes to p53-independent apoptosis following IR (Figure 1, B–F).

All IR-induced acridine orange and anti-C3 staining was blocked at both early and late time points in wing discs mutant for the caspase-9 homolog *dronc* (Figure S1B and Figure S2D), indicating that *dronc* is required for both p53-dependent and p53-independent apoptosis. Similarly, in discs expressing the anti-apoptotic baculovirus protein p35, which inhibits the effector caspases Drice and DCP-1 (XUE and HORVITZ 1995; KONDO *et al.* 2006; XU *et al.* 2006; BAUM *et al.* 2007; LANNAN *et al.* 2007), no acridine orange staining was observed at any time point (Figure S2E). Because p35 inhibits effector caspase activity after proteolytic cleavage, cleaved caspase-3 staining can still be observed once these caspases are activated (YU *et al.* 2002). When p35 is expressed in the posterior half of wild-type or *p53* mutant wing discs, IR-induced caspase staining is induced in both halves, but the staining is delayed in the p35-expressing region (Figure S1, C and D).

Induction of HID by IR was examined in *p53* mutant discs expressing p35, which allows HID to accumulate without causing cell death. HID induction is observed 16 and 24 hr following irradiation of *p53* mutant cells expressing p35 (Figure 2A, posterior cells). Overall, our analysis of *hid* and caspase function indicates that p53-independent apoptosis following IR utilizes the same core apoptotic machinery activated in response to most developmental and cell stress signals in Drosophila.

Regulation of p53-independent apoptosis by the JNK pathway: Following IR, JNK signaling is activated in a p53-dependent manner and inhibition of JNK signaling

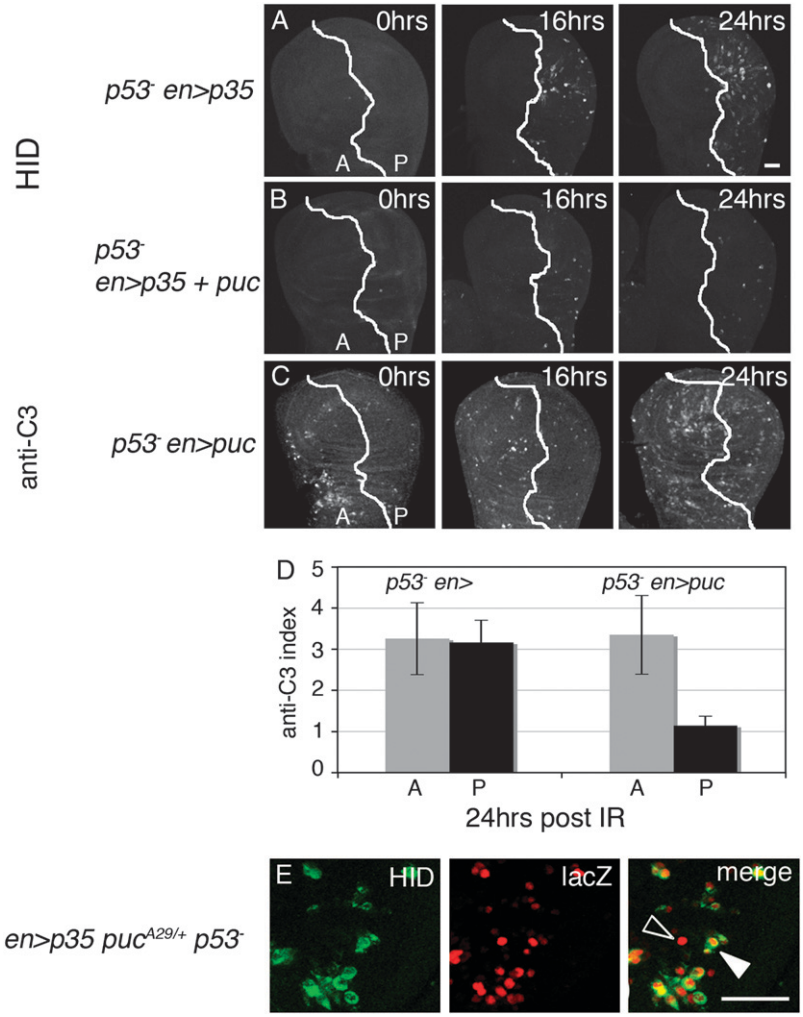

FIGURE 2.—The JNK pathway regulates p53-independent induction of HID and apoptosis following IR. (A) HID levels are increased following irradiation of *p53* mutant wing discs cells. The white line marks the boundary between anterior (left) and posterior (right). The baculovirus anti-apoptotic protein p35 is expressed in posterior cells using UAS-p35 and an *engrailed*-Gal4 driver. Bar, 50 μm. (B) Induction of HID by irradiation is blocked in *p53* mutant cells that express the JNK inhibitor *puc*. (C) *puc* expression reduces induction of p53-independent apoptosis following IR. Apoptosis is assayed by anti-C3 staining. (D) Quantification of anti-C3 staining in *p53* mutant cells compared to *p53* mutant cells overexpressing *puc* in the posterior. For each genotype, levels of anti-C3 staining were quantified in the anterior (A) and posterior (P) in five discs. Posterior anti-C3 staining is significantly reduced in the discs overexpressing *puc* ($n = 5$, *P*-value <0.01). (E) At higher magnification, irradiation-induced HID (green) and *puc-lacZ* (red) are expressed in overlapping cells in the posterior of *puc-lacZ*/+ *p53* mutant wings discs expressing p35. Most stained cells express both *puc-lacZ* and HID (open arrowhead). Some cells express *puc-lacZ*, but not HID (solid arrowhead). Bar, 20 μm.

reduces induction of apoptosis (McEwen and Peifer 2005). The Drosophila JNK signaling pathway also regulates apoptosis in response to other cellular stresses, including UV irradiation (Jassim *et al.* 2003; Luo *et al.* 2007), abnormal expression patterns of the DPP or WG morphogens (Adachi-Yamada *et al.* 1999; Adachi-Yamada and O'Connor 2002), or reduced dosage of ribosomal protein genes (Moreno *et al.* 2002).

The role of JNK signaling in p53-independent induction of HID by IR was examined using *puc*, a JNK target gene encoding a JNK phosphatase. *puc* acts in a negative feedback loop to limit JNK signaling and can be used to efficiently block JNK activity when overexpressed in a specific cell type or region (Martin-Blanco *et al.* 1998). *puc* overexpression in *p53* mutant discs reduced HID induction after IR (compare posterior compartments in Figure 2, A and B). *puc* overexpression also reduces anti-C3 staining following IR (Figure 2, C and D); the ratio of posterior to anterior anti-C3 staining is 1.4 in *p53* mutant discs and is reduced to 0.3 in *p53* mutant discs overexpressing *puc* in the posterior. The incomplete inhibition of apoptosis in these discs may indicate that a JNK-independent pathway also contributes to this response.

A *puc-lacZ* reporter, puc^{A29}, was used to monitor JNK signaling in irradiated discs (Martin-Blanco *et al.* 1998; Kanda and Miura 2004). As previously reported (McEwen and Peifer 2005), p53-dependent expression of the *puc* reporter is observed 4 hr following IR (data not shown). However, *p53* mutant discs begin expressing the reporter at later time points following IR (Figure 3A). In irradiated *p53* mutant wing discs expressing p35, HID and the *puc* reporter are expressed in an overlapping set of cells (Figure 2E).

Cells heterozygous for *puc* mutations exhibit hyperactivation of the JNK pathway (Martin-Blanco *et al.* 1998), indicating that *puc* gene dosage is rate limiting for JNK activity. If the level of JNK activation determines the amount of p53-independent apoptosis, then *p53* mutant discs heterozygous for *puc* mutations should exhibit increased apoptosis following irradiation. At 16 and 24 hr after IR, there is a 3- and 4-fold increase in caspase staining in *p53* mutant discs that are also heterozygous for *puc* compared to *p53* single-mutant

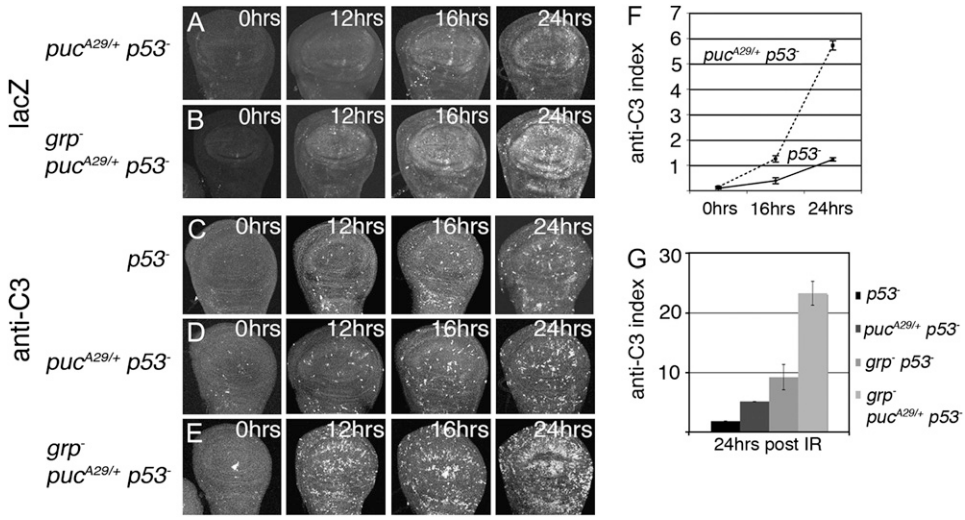

FIGURE 3.—*grp* and *puc* limit p53-independent apoptosis following IR. (A) *lacZ* expression is increased following irradiation of $puc^{A29/+}$ *p53* mutant wing discs. puc^{A29} is an enhancer trap line in which the *lacZ* reporter is inserted in the *puc* locus. (B) Induction of *lacZ* is stronger and faster in *grp* $puc^{A29/+}$ *p53* mutant discs, which are defective for G_2 arrest following IR. (C–E) Apoptosis was assayed using anti-C3. (C and D) *puc/+, p53* mutant discs have increased apoptosis compared to *p53* single-mutant discs. (E) Triple-mutant *grp puc-lacZ/+ p53* mutant discs have increased apoptosis compared to either *puc/+ p53* or *grp p53* double-mutant discs (see Figure 4F). (F) Quantification of anti-C3 staining in *puc/+ p53* and *p53* mutant discs. (G) Quantification of anti-C3 staining in *p53* single-mutant discs, *puc/+ p53* or *grp p53* double-mutant discs, and *grp puc-lacZ/+ p53* triple-mutant discs. Apoptosis was examined 24 hr following IR treatment. For each disc and data point, at least five wing discs were examined. Error bars indicate the standard error of the mean.

discs (Figure 3, C, D, and F). The overall correlation of *puc* expression levels and apoptosis suggests that the JNK pathway helps regulate p53-independent apoptosis following IR.

Drosophila Chk1 is a negative regulator of p53-independent apoptosis following IR: The induction of p53-independent apoptosis following IR correlates with cell cycle progression. IR-induced G_2 delay in the wing disc lasts up to 8 hr and requires the Drosophila *chk1* kinase homolog *grp* (FOGARTY *et al.* 1997; BRODSKY *et al.* 2000a), even in the absence of p53 or MNK function (Figure 4, A–D). While IR-induced apoptosis in wild-type discs begins during the cell cycle arrest period (within 3–4 hr), apoptosis in *p53* mutant discs is largely observed after mitosis has resumed. In *grp p53* double-mutant discs, which fail to arrest in G_2, increased levels of apoptosis are observed at 12 and 16 hr compared to *p53* single-mutant discs (Figure 4, E, F, and I). Similarly, apoptosis is increased in *grp mnk* double-mutant wing discs compared to *mnk* single-mutant discs (Figure 4, G, H, and J). Previous studies have established that mutations in *mnk* and *grp* do not affect the frequency of chromosome breaks following IR (JAKLEVIC and SU 2004; OIKEMUS *et al.* 2006), indicating that the increased apoptosis is due to a defect in cell cycle arrest, not simply an increase in unrepaired DNA breaks.

In mammalian cells that lack both p53 and Chk1 function, DNA damage can induce a type of mitotic catastrophe in which the mitotic marker phosphohistone H3 and cleaved caspase-3 are present simultaneously in the dying cells (REINHARDT *et al.* 2007). However, in irradiated *grp p53* mutant wing discs, these markers label two separate cell populations: mitotic cells stained with anti-phosphohistone H3 are predominantly in the apical region of the disc, while apoptotic cells stained with anti-cleaved caspase-3 are largely found in the basal region (Figure 5, A and B). These results suggest that these cells do not undergo apoptosis while in M-phase.

The relationship between *grp* and *puc* during p53-independent apoptosis was also examined. IR-induced expression of the *puc* reporter is faster and stronger in *grp p53* double-mutant discs compared to *p53* single-mutant discs (Figure 3, A and B), suggesting that cell cycle arrest normally helps delay induction of JNK signaling. The effect of both inactivating cell cycle arrest and reducing the level of negative feedback signaling by *puc* was also examined: *grp puc/+ p53* triple-mutant discs have higher levels of apoptosis than either *grp p53* or *puc/+ p53* double-mutant discs (Figure 3, D–G). Thus, while the inactivation of cell cycle delay accelerates the formation of cells with elevated JNK signaling, decreasing the negative feedback signal from *puc* can further increase the number of cells that undergo p53-independent apoptosis following IR.

p53-independent apoptosis reduces the number of aneuploid cells recovered following IR: The role of p53-dependent and p53-independent apoptosis in maintaining genomic integrity was examined using an assay based on haploinsufficiency of ribosomal protein genes. In animals exposed to IR or with mutations in DNA repair loci, somatic mutations scored by loss of heterozygosity (LOH) are typically accompanied by loss of multiple genetic markers and the *Minute* phenotype, caused by haploinsufficiency of ribosomal protein genes (BAKER *et al.* 1978). These results indicate that most LOH was due to segmental aneuploidy (loss of large chromosomal regions) rather than induction of point mutations or mitotic recombination. To probe genetic loss across the entire genome, we scored the frequency of

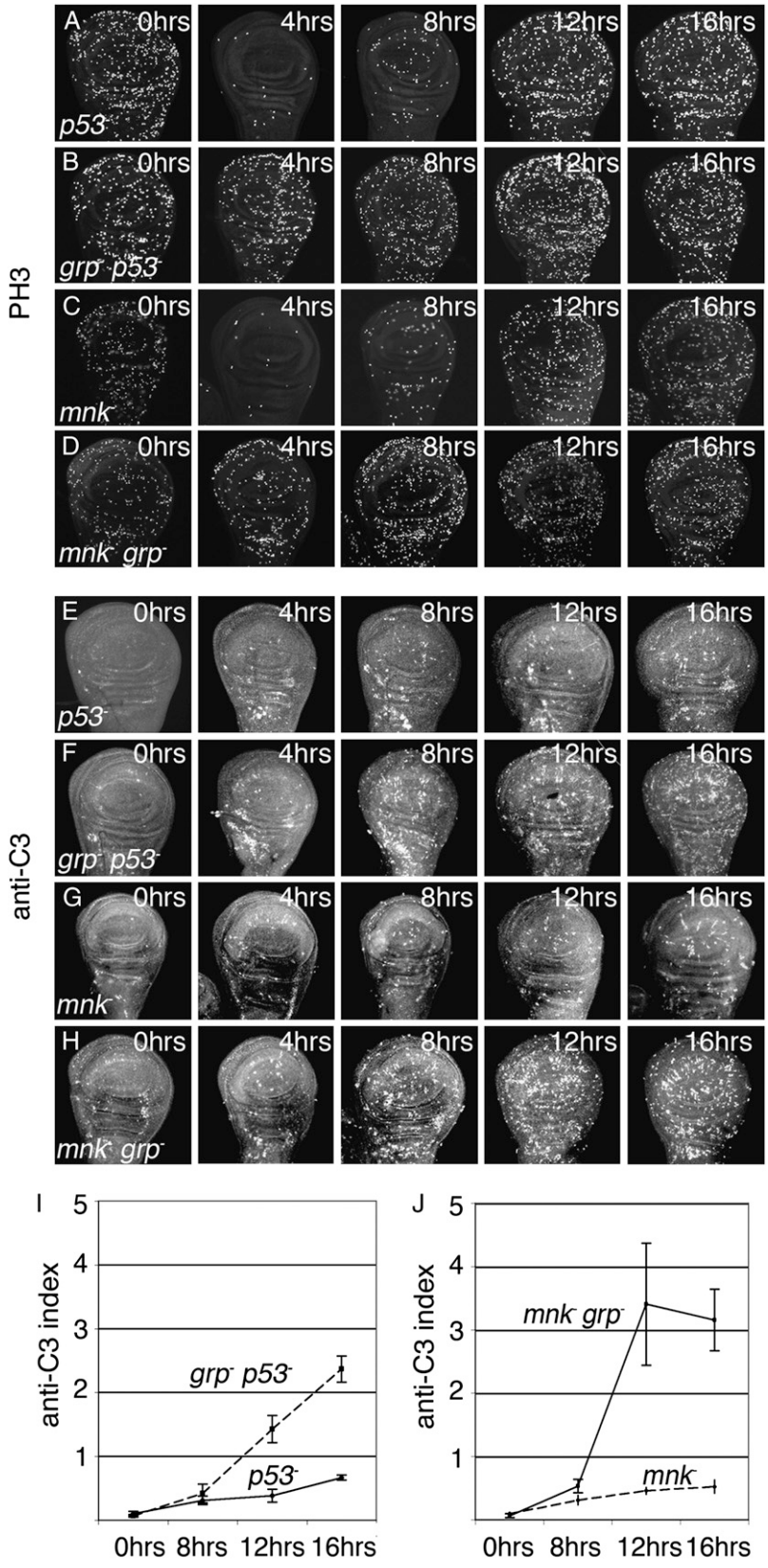

FIGURE 4.—*grp* mutations enhance MNK and p53-independent apoptosis following irradiation. (A–D) Developing wing discs were stained following IR with anti-phospho-Ser10 histone H3 (PH3) to detect mitotic cells. Mitotic entry is largely blocked at 4 and 8 hr following IR in *mnk* and *p53* single-mutant wing discs, but not in *grp p53* or *mnk grp* double-mutant discs. (E–H) Apoptosis was assayed in *p53* and *mnk* single-mutant and *grp p53* and *mnk grp* double-mutant imaginal wing discs by staining with anti-C3. *grp p53* and *mnk grp* double-mutant discs have increased apoptosis compared to *p53* and *mnk* single-mutant discs. (I and J) Anti-C3 staining was quantified at 0, 8, 12, and 16 hr after treatment with IR. Double-mutant discs lacking the cell cycle checkpoint gene *grp* have elevated irradiation-induced staining compared to single mutants ($n = 5$). Error bars indicate the standard error of the mean.

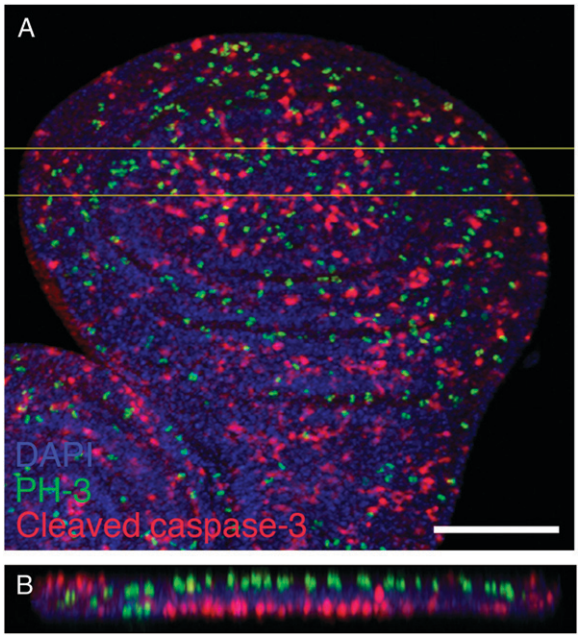

Figure 5.—p53-independent apoptosis is not activated in cells that are actively progressing through mitosis. (A) An *X–Y* view of a confocal *z*-series of a *grp p53* mutant wing disc, 16 hr after IR, stained with anti-C3 (red), PH3 (green), and DAPI (blue). (B) *X–Z* cross-section of the same wing disc at the region marked with yellow lines above. Little or no overlap of apoptotic and mitotic cells is observed.

Minute cells following IR. Because the 65 *Minute* loci are spread throughout the euchromatic genome (Marygold *et al.* 2007), reduced copy number of most large genomic regions is likely to result in the *Minute* phenotype. Previous studies have used this phenotype to assay the genetic consequences of diverse sources of chromosome damage, including mutations in telomere protection genes (Oikemus *et al.* 2004, 2006), telomere loss due to dicentric chromosomes (Ahmad and Golic 1999), mutations in DNA damage response and repair genes (Brodsky *et al.* 2000b; Johnson-Schlitz *et al.* 2007), and induction of DNA breaks by *P*-element mobilization (Engels *et al.* 1987). These studies confirm that induction of *Minute* bristles following IR is due to chromosome damage rather than other types of cellular damage. It is possible that a small percentage of defective bristles are not due to induction of aneuploidy, but these events would probably reflect other types of genetic damage, such as *Minute* gene point mutations.

Minute cells were scored in adults following X-irradiation of early third instar larvae. If apoptosis reduces the number of IR-induced aneuploid cells, then inhibiting apoptosis should increase the number of these cells that survive to adulthood. Following irradiation of wild-type larvae with 1000 rad, 2% of bristles exhibit the *Minute* phenotype (Figure 6, A and C). No difference in the number of defective bristles was seen in *p53* mutant compared to wild-type animals at either dose, indicating that p53-dependent apoptosis is not essential to eliminate *Minute* cells following IR (Figure 6C). This result is inconsistent with a previous study, in which an increase in *Minute* bristles was reported following IR of late third instar larvae (Lee *et al.* 2003). When we repeated this experiment using the later stage, there was still no significant increase in *Minute* bristles in *p53* mutant animals (Figure S3A). To help control for differences in genetic background, additional wild-type and *p53* mutant lines were tested. Again, no increase in *Minute* bristles was observed in *p53* mutants compared to wild-type lines (Figure S3B). It is possible that the previously reported increase was due to a second mutation on the *p53* mutant chromosome.

Elimination of aneuploid cells by p53-independent apoptosis could compensate for the apoptotic defect in *p53* mutant animals. To test if *p53*-independent apoptosis helps limit IR-induced aneuploidy, the frequency of IR-induced *Minute* bristles was also examined in *hid p53* double-mutant animals. At 1000 rad, the frequency increased from 2% in *p53* single-mutant animals to 5% in double mutants (Figure 6, B and C). Thus, in a *p53* mutant background, the p53-independent apoptosis induced by IR is required to limit genomic instability as measured by the appearance of adult cells heterozygous for a *Minute* mutation. If bristle cells are representative of the ~50,000 cells in the developing wing, then ~2500 (5% of 50,000) *Minute* cells are induced by IR per disc and ~1500 (3% of 50,000) are eliminated by apoptosis in a *p53* single-mutant disc, but not in a *p53 hid* double-mutant wing disc.

hid is a target of both p53-dependent and p53-independent signaling following DNA damage. In *hid* single mutants, IR-induced apoptosis is eliminated at early time points, but only partly reduced at later time points (Figures 1 and Figure S2F), a phenotype that is intermediate between *p53* single- and *hid p53* double-mutant animals. The increased frequency of *Minute* cells in IR-treated *hid p53* double mutants compared to *hid* single mutants indicates that p53 helps limit the appearance of aneuploid cells when p53-independent apoptosis is also blocked (Figure 6C).

Altered *brk* expression following IR: To explore if IR broadly disrupts patterned gene expression in the developing wing, we examined the expression of several key regulators of wing patterning. Following DNA damage, missegregation of rearranged or broken chromosomes during mitosis generates cells with segmental aneuploidy. Reduced copy number of haploinsufficient genes, such as the *Minute* genes, could lead to altered gene expression and apoptosis. Phenotypes associated with *Minute* cells in the wing disc include increased apoptosis, JNK pathway activation, and ectopic expression of the transcriptional repressor *brinker* (*brk*) due to reduced signaling by the *dpp* signaling pathway (Moreno *et al.* 2002; Tyler *et al.* 2007). Whereas both JNK and apoptosis are activated by many different types of cellular

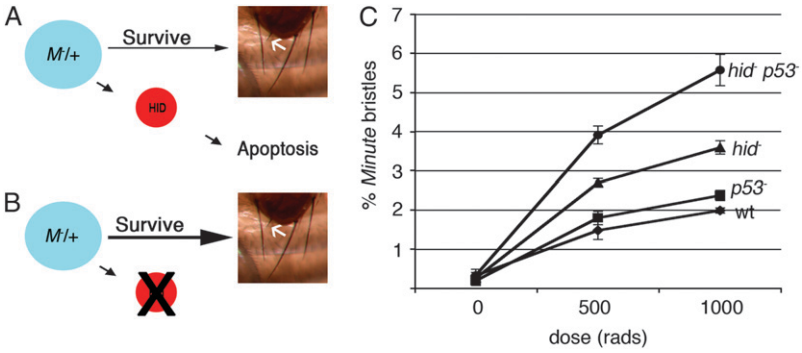

FIGURE 6.—p53-independent apoptosis limits the accumulation of *Minute* cells following irradiation. (A) Aneuploid cells with the *Minute* phenotype are induced following irradiation of a *p53* mutant wing disc. Some of these cells are eliminated by *hid*-dependent apoptosis, while others survive and differentiate into adult cell types. Adult bristles form a stereotypic pattern on the notum of an untreated, wild-type animal. An example of an adult bristle exhibiting the *Minute* phenotype (shorter and thinner) is indicated with an arrow. (B) In *hid p53* double-mutant animals, more IR-induced *Minute* cells escape apoptosis and survive to adulthood. (C) The frequency of *Minute* bristles induced by IR is higher in *hid* single mutants and *hid p53* double-mutant animals compared to wild-type or *p53* single-mutant animals. A total of 60 animals were scored for each genotype in three independent experiments ($n = 3$, *P*-value <0.01). Error bars indicate the standard error of the mean.

stresses, including altered gene expression patterns (UMEMORI *et al.* 2009), *brk* may be more specific for *dpp* signaling. *brk* expression is normally repressed in the center of developing wing discs and gradually increases toward the anterior and posterior edges of the disc (*brk-lacZ* in Figure 7, A–C). At 24 hr following IR, individual cells in the center of *p53* mutant discs ectopically express *brk* and expression in the lateral regions becomes more irregular (Figure 7, A–C). Inhibition of apoptosis by p35 expression increases the number of cells with ectopic *brk* expression. An average of 9 cells ectopically express high levels of *brk* in the center of the *p53* mutant wing discs expressing p35 (SEM = 2.6, $n = 5$ discs, *P*-value <0.01, treated compared with untreated), while an average of 2.6 cells ectopically express *brk* without p35 (SEM = 1.7, $n = 5$, *P*-value <0.01, treated compared with untreated). (These numbers significantly underestimate the total number of cells with abnormal *brk* expression since we excluded cells within or adjacent to the normal *brk* expression domain in our analysis.) Ectopic *brk* expression following IR is also observed in wild-type discs, suggesting that induction of this phenotype by IR can occur in parallel to p53-dependent apoptosis (Figure S4). In wild-type discs, p53-dependent apoptosis is induced within 4 hr of X-irradiation, but ectopic expression of *brk* is not observed at this time point (data not shown), indicating that altered *brk* expression is not a secondary consequence of induced apoptosis. Because ectopic *brk* expression is sufficient to activate JNK-dependent apoptosis (MARTIN *et al.* 2004), the observed changes in *brk* expression could contribute to the elimination of *Minute* cells (MORENO *et al.* 2002).

Although ectopic expression of *brk* is consistent with the generation of *Minute* cells, it could alternatively reflect altered expression of genes that act earlier in the anterior–posterior patterning hierarchy or reflect a widespread disruption of patterned gene expression following cellular damage by IR. The expression patterns of three additional gene products, two with restricted expression along the anterior–posterior axis (EN and PTC) and one with restricted expression along the dorsal–ventral axis (WG), were also examined in irradiated *p53* mutant wing discs; no change in expression was observed for any of these proteins (Figure 7, D–F). This small-scale survey suggests that irradiation does not generally disrupt developmental networks and that the effect on *brk* expression is not due to loss of the anterior–posterior compartment (reflected by EN expression) or aberrant activity of the Hedgehog pathway along the compartment boundary (reflected by PTC expression).

DISCUSSION

While p53 plays a conserved role connecting the DNA damage response pathway to the core apoptotic machinery, there are also p53-independent mechanisms to induce cell death following chromosome damage. We find that this p53-independent response in Drosophila requires the pro-apoptotic gene *hid*, the apical caspase *dronc*, and downstream effector caspases. Proper regulation of the JNK phosphatase *puc* is required for the full induction of *hid* expression and apoptosis following irradiation of *p53* mutant discs. *puc* and the cell cycle checkpoint gene *grp* are negative regulators of this response and mutations in these genes act additively to sensitize *p53* mutant cells to IR. This response plays an important *in vivo* role in limiting the accumulation of aneuploid cells following IR. We propose that p53-independent apoptosis reflects a second, indirect mechanism that acts in parallel to the canonical DNA damage response pathway to eliminate cells with altered genomes following IR (Figure 8): in this model, incorrect repair of IR-induced chromosome breaks generates cells with segmental aneuploidy, resulting in haploinsufficiency of genes required for cell survival.

IR-induced apoptosis without components of the canonical DNA damage response pathway: The ATM/Chk2/p53 signaling module is activated by local disruptions in chromatin structure following DNA damage

and plays a central role in IR-induced apoptosis. In mammalian cells lacking p53, components of the DNA damage response pathway, such as ATR and p73, have been implicated in damage-induced apoptosis (Roos and Kaina 2006; Sidi *et al.* 2008). In this study and previous work (Oikemus *et al.* 2004, 2006; Wichmann *et al.* 2006; Titen and Golic 2008), genetic analysis of single and double mutants in components of the Drosophila DNA damage response pathway suggests that chromosome damage can induce apoptosis through a mechanism that does not utilize this pathway. Consistent with these results, activation of ATM and ATR kinases following IR (as measured by phospho-H2Av staining) largely subsides within a few hours of IR in embryos (Kusch *et al.* 2004) and discs (our unpublished results), well before increased p53-independent apoptosis, JNK target gene expression, or HID.

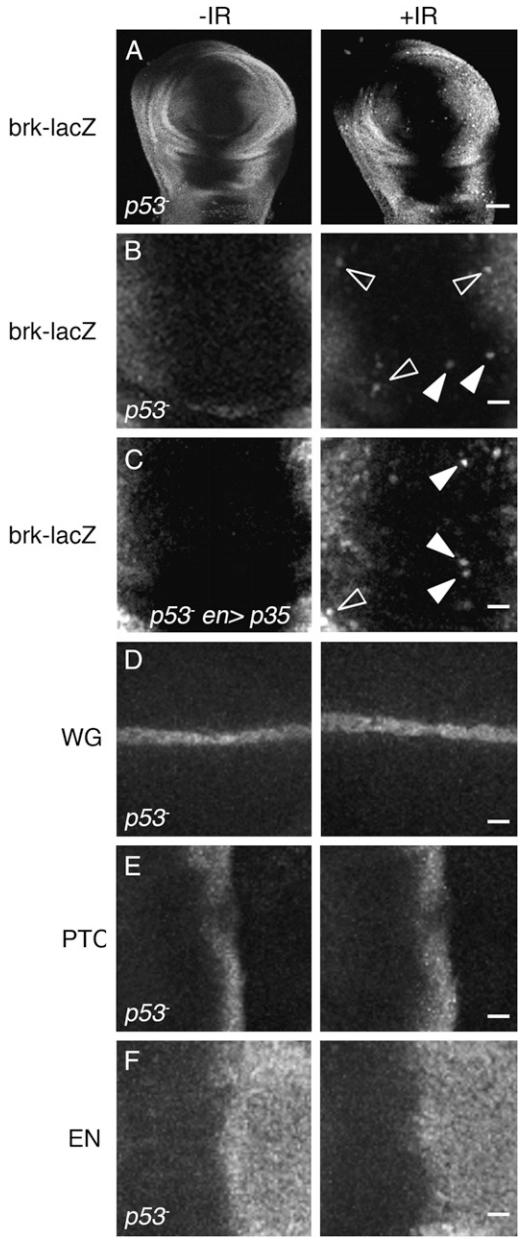

Furthermore, in a recent study using dicentric chromosomes to induce chromosome breaks and telomere loss, all dicentric chromosomes could induce p53-dependent apoptosis, but only dicentric chromosomes that led to aneuploidy could induce p53-independent apoptosis (Titen and Golic 2008).

In *p53* or *mnk* mutant discs, IR-induced apoptosis is observed only after cells have recovered from damage-induced cell cycle delay. This response is accelerated in double-mutant discs that fail to arrest due to mutations in the Drosophila *chk1* homolog *grp*. Similarly, p53-independent induction of *puc* by IR is observed after resumption of cell cycle progression in single-mutant discs and is accelerated by loss of *grp*. Inhibition of JNK signaling by overexpression of *puc* substantially reduces p53-independent induction of HID and apoptosis, suggesting that this response is partly dependent on the JNK pathway. The remaining apoptosis may either reflect incomplete inhibition of JNK signaling by *puc* overexpression or suggest that an alternative pathway acts in parallel to JNK to promote a lower level of p53-independent apoptosis. While the only described function of *puc* to date is as an inhibitor of JNK signaling, we cannot rule out the possibility that inhibition of other pathways by *puc* contributes to the regulation of p53-independent apoptosis. Overall, these results suggest that cell cycle arrest helps delay p53-independent activation of JNK signaling and apoptosis following IR.

Regulation of genomic stability by p53-dependent and -independent responses: p53-dependent apoptosis is hypothesized to help preserve genome stability by rapidly eliminating cells with severe chromosome damage. In mouse models with elevated genomic instability, loss of p53 function further increases tumorigenesis (Attardi 2005). However, temporal analysis of mouse p53 function following irradiation suggests that the DNA damage response function of p53 may not be

Figure 7.—*brk* is ectopically expressed following irradiation. (A) A *lacZ* enhancer trap reporter inserted at the *brk* locus is used to monitor *brk* expression. Without IR, *brk* is expressed at elevated levels in the anterior (left) and posterior (right) regions of the developing wing and at lower levels in the central region. Bar, 50 μm. (A) Twenty-four hours following IR, ectopic *lacZ* expression is observed in the medial region of *brk-lacZ/+ p53*$^{-}$ discs and more irregular *lacZ* expression is observed in the lateral regions. (B) Higher magnification of the medial region of a *brk-lacZ/+ p53*$^{-}$ wing disc. Imaginal discs treated with IR contain cells ectopically expressing *brk*. Medial cells that expressed *brk* and were clearly separate from the normal expression domain (solid arrowheads) were used to quantify ectopic *brk* expression. This is an underestimate since medial cells with inappropriate levels of *lacZ* expression were not scored if they were within or adjacent to the normal *brk* expression domain (open arrowheads). Bar, 20 μm. (C) More cells with ectopic *brk* expression were observed following irradiation of *brk-lacZ/+ p53*$^{-}$ wing discs expressing the anti-apoptotic protein p35. (D–F) Ectopic expression of Wingless, Patched, or Engrailed protein was not observed following IR. For each genotype five wing discs were scored.

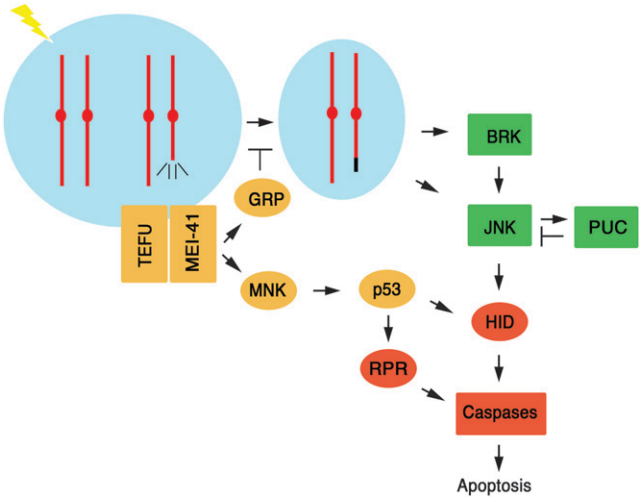

Figure 8.—Model for p53-dependent and p53-independent apoptosis. In response to DNA damage, cells sense DNA breaks and activate repair, cell cycle delay, and apoptosis. Following DNA damage, TEFU/dATM and MEI-41/dATR kinases activate MNK/dChk2 and p53 to induce apoptosis (orange boxes). p53 regulates the pro-apoptotic genes *hid* and *rpr*, resulting in caspase activation (red box). GRP/dChk1 promotes cell cycle delay, allowing time for DNA repair. Incorrect repair of chromosome breaks followed by progression through mitosis will result in cells with reduced copy number of large chromosome regions (segmental aneuploidy). Haploinsufficiency of genes encoding ribosomal proteins or other products can induce apoptosis by ectopic *brk* expression, JNK pathway activation, and induction of *hid* expression. Other apoptotic mechanisms may also act to remove aneuploid cells (not shown).

critical for tumor suppression (Christophorou *et al.* 2006).

In Drosophila, the role of p53 in limiting genomic instability appears to depend on the source of DNA damage or the type of genetic alterations assayed. In one study, telomere loss following dicentric chromosome formation led to an extremely high frequency of larval neuroblasts with abnormal karyotypes; p53 helped reduce the number of abnormal cells over time (Titen and Golic 2008). Another study using a genetic assay for LOH at the *multiple wing hair* (*mwh*) locus reported increased LOH following IR in *p53* mutant animals (Sogame *et al.* 2003), a result we have confirmed with an independently derived *p53* allele (Figure S5). However, when using the *Minute* assay to examine genomic instability, we found that p53 function was not essential to limit IR-induced aneuploidy, despite the very high levels of p53-dependent apoptosis normally induced following IR. Several factors might account for the different conclusions reached using these assays. In the *mwh* assay, two types of genetic damage not associated with aneuploidy, small deletions or mitotic recombination, can be recovered that may not be scored in the *Minute* assay. p53-independent apoptosis may be able to compensate in the absence of p53 function to eliminate aneuploid cells, while p53-dependent apoptosis may play a more critical role in eliminating cells with genetic damage that is not associated with aneuploidy. Consistent with this interpretation, we find that p53 does contribute to genomic stability in the *Minute* assay when the p53-independent response is blocked (compare *hid* single-mutant to *hid p53* double-mutant animals).

We find a significant increase in the number of aneuploid cells recovered following IR when both p53-dependent and p53-independent apoptosis are blocked. Inhibition of both pathways results in a 2.5-fold increase in adult bristle cells with the *Minute* phenotype, resulting in 5% of bristle cells exhibiting this severe morphological defect. These results demonstrate that p53-independent apoptosis plays an important functional role following IR by substantially reducing the eventual number of adult aneuploid cells. Because *hid* mutations affect both p53-dependent and p53-independent apoptosis, we cannot determine whether this response is required for genomic stability in cells with the normal p53 signaling pathway.

Aneuploidy as a possible apoptotic signal following IR: A key unresolved question in this study is what signal activates p53-independent *puc* and *hid* expression and apoptosis following IR. An attractive possibility is that aneuploidy itself is the signal. In strong support of this hypothesis, induction of p53-independent apoptosis following telomere loss is observed only if the resulting broken chromosome can lead to aneuploidy (Titen and Golic 2008). Our analysis of IR-induced *Minute* bristles indicates that many aneuploid cells are generated following IR and then eliminated by apoptosis. In larvae, chromosome rearrangements appear shortly after IR (Gatti *et al.* 1974). IR-induced changes in the expression of *brk*, *puc*, and *hid* are consistent with the production of aneuploid cells exhibiting the *Minute* phenotype, although these markers are not specific for aneuploid cells. Since haploinsufficiency of the widely distributed *Minute* genes is sufficient to induce apoptosis (Moreno *et al.* 2002; Coelho *et al.* 2005) and induction of spontaneous apoptosis in *Minute* heterozygous animals does not require p53 (L. M. McNamee, unpublished results), this mechanism should eventually be activated in aneuploid cells induced by IR. While *Minute* genes represent the primary source of loci that are haploinsufficient for normal growth (Lindsley *et al.* 1972; Marygold *et al.* 2007), it is also possible that the cumulative effect of reduced dosage of many genes in aneuploid cells disrupts normal gene expression and cell survival. On the basis of these observations, we propose that DNA damage indirectly induces apoptosis by creating chromosome aberrations leading to segmental aneuploidy and activating JNK-dependent and p53-independent apoptosis (Figure 8). However, we cannot easily rule out the possibility that an additional response to IR could kill these cells before apoptosis due to aneuploidy is activated.

Haploinsufficiency of ribosomal genes could contribute to damage-induced apoptosis in vertebrates as well. In mice heterozygous for ribosomal protein gene mutations, both p53-dependent and p53-independent signaling are induced, leading to increased apoptosis and reduced growth (Panic *et al.* 2006; Danilova *et al.* 2008). Diamond Blackfan anemia (DBA) is linked to haploinsufficiency of human ribosomal protein genes (Draptchinskaia *et al.* 1999; Gazda and Sieff 2006; Gazda *et al.* 2006; Cmejla *et al.* 2007; Choesmel *et al.* 2008) and is associated with increased cell death (Flygare and Karlsson 2007). As in Drosophila, mammalian ribosomal protein genes are widely distributed throughout the genome. Thus, genetic or environmental changes resulting in aneuploidy should frequently induce the cellular responses associated with ribosomal protein gene haploinsufficiency.

In summary, we have identified a p53-independent pathway that limits the formation of aneuploid cells through JNK- and HID-dependent apoptosis. We hypothesize that rather than detect damaged chromosomes directly, this mechanism is activated by the reduced dosage of critical loci, such as ribosomal protein genes, in aneuploid cells.

Inactivation of this response causes an increase in visibly defective bristle cells following DNA damage. Thus, in Drosophila, this mechanism helps eliminate cells that would reduce the fitness of the adult animal. We have shown that mutations in a cell cycle checkpoint gene and a JNK phosphatase enhance this response following IR. These and other components of this pathway may provide useful targets to reduce the proliferation of aneuploid cancer cells or to sensitize cancer cells to the effects of DNA-damaging agents.

We especially thank Hyung Don Ryoo for providing polyclonal antibody to HID. We also thank Bruce Hay, Hermann Stellar, Andreas Bergmann, Gerard Campbell, Takashi Adachi-Yamada, and the Bloomington Stock Center for providing Drosophila stocks. We thank Neal Silverman, Steve Grossman, and Eric Baehrecke for comments on the manuscript. We thank Simon Titen and Kent Golic for sharing their results prior to publication. This work was supported by a New Scholar in Aging Award from the Ellison Medical Foundation and by a grant from the American Cancer Society (RSG-05-026-01-CCG).

LITERATURE CITED

Abdelwahid, E., T. Yokokura, R. J. Krieser, S. Balasundaram, W. H. Fowle *et al.*, 2007 Mitochondrial disruption in Drosophila apoptosis. Dev. Cell **12:** 793–806.

Abrams, J. M., K. White, L. I. Fessler and H. Steller, 1993 Programmed cell death during Drosophila embryogenesis. Development **117:** 29–43.

Adachi-Yamada, T., and M. B. O'Connor, 2002 Morphogenetic apoptosis: a mechanism for correcting discontinuities in morphogen gradients. Dev. Biol. **251:** 74–90.

Adachi-Yamada, T., K. Fujimura-Kamada, Y. Nishida and K. Matsumoto, 1999 Distortion of proximodistal information causes JNK-dependent apoptosis in Drosophila wing. Nature **400:** 166–169.

Ahmad, K., and K. G. Golic, 1999 Telomere loss in somatic cells of Drosophila causes cell cycle arrest and apoptosis. Genetics **151:** 1041–1051.

Akdemir, F., A. Christich, N. Sogame, J. Chapo and J. M. Abrams, 2007 p53 directs focused genomic responses in Drosophila. Oncogene **26:** 5184–5193.

Attardi, L. D., 2005 The role of p53-mediated apoptosis as a crucial anti-tumor response to genomic instability: lessons from mouse models. Mutat. Res. **569:** 145–157.

Baker, B. S., A. T. Carpenter and P. Ripoll, 1978 The utilization during mitotic cell division of loci controlling meiotic recombination and disjunction in Drosophila melanogaster. Genetics **90:** 531–578.

Bartek, J., and J. Lukas, 2007 DNA damage checkpoints: from initiation to recovery or adaptation. Curr. Opin. Cell Biol. **19:** 238–245.

Baum, J. S., E. Arama, H. Steller and K. McCall, 2007 The Drosophila caspases Strica and Dronc function redundantly in programmed cell death during oogenesis. Cell Death Differ. **14:** 1508–1517.

Bergmann, A., A. Y. Yang and M. Srivastava, 2003 Regulators of IAP function: coming to grips with the grim reaper. Curr. Opin. Cell Biol. **15:** 717–724.

Bi, X., S. C. Wei and Y. S. Rong, 2004 Telomere protection without a telomerase; the role of ATM and Mre11 in Drosophila telomere maintenance. Curr. Biol. **14:** 1348–1353.

Bi, X., D. Srikanta, L. Fanti, S. Pimpinelli, R. Badugu *et al.*, 2005 Drosophila ATM and ATR checkpoint kinases control partially redundant pathways for telomere maintenance. Proc. Natl. Acad. Sci. USA **102:** 15167–15172.

Brodsky, M. H., W. Nordstrom, G. Tsang, E. Kwan, G. M. Rubin *et al.*, 2000a Drosophila p53 binds a damage response element at the reaper locus. Cell **101:** 103–113.

Brodsky, M. H., J. J. Sekelsky, G. Tsang, R. S. Hawley and G. M. Rubin, 2000b mus304 encodes a novel DNA damage checkpoint protein required during Drosophila development. Genes Dev. **14:** 666–678.

Brodsky, M. H., B. T. Weinert, G. Tsang, Y. S. Rong, N. M. McGinnis *et al.*, 2004 Drosophila melanogaster MNK/Chk2 and p53 regulate multiple DNA repair and apoptotic pathways following DNA damage. Mol. Cell. Biol. **24:** 1219–1231.

Chew, S. K., F. Akdemir, P. Chen, W. J. Lu, K. Mills *et al.*, 2004 The apical caspase dronc governs programmed and unprogrammed cell death in Drosophila. Dev. Cell **7:** 897–907.

Choesmel, V., S. Fribourg, A. H. Aguissa-Toure, N. Pinaud, P. Legrand *et al.*, 2008 Mutation of ribosomal protein RPS24 in Diamond-Blackfan anemia results in a ribosome biogenesis disorder. Hum. Mol. Genet. **17:** 1253–1263.

Christich, A., S. Kauppila, P. Chen, N. Sogame, S. I. Ho *et al.*, 2002 The damage-responsive Drosophila gene sickle encodes a novel IAP binding protein similar to but distinct from reaper, grim, and hid. Curr. Biol. **12:** 137–140.

Christophorou, M. A., I. Ringshausen, A. J. Finch, L. B. Swigart and G. I. Evan, 2006 The pathological response to DNA damage does not contribute to p53-mediated tumour suppression. Nature **443:** 214–217.

Ciapponi, L., G. Cenci, J. Ducau, C. Flores, D. Johnson-Schlitz *et al.*, 2004 The Drosophila Mre11/Rad50 complex is required to prevent both telomeric fusion and chromosome breakage. Curr. Biol. **14:** 1360–1366.

Ciapponi, L., G. Cenci and M. Gatti, 2006 The Drosophila Nbs protein functions in multiple pathways for the maintenance of genome stability. Genetics **173:** 1447–1454.

Cmejla, R., J. Cmejlova, H. Handrkova, J. Petrak and D. Pospisilova, 2007 Ribosomal protein S17 gene (RPS17) is mutated in Diamond-Blackfan anemia. Hum. Mutat. **28:** 1178–1182.

Coelho, C. M., B. Kolevski, C. Bunn, C. Walker, A. Dahanukar *et al.*, 2005 Growth and cell survival are unevenly impaired in pixie mutant wing discs. Development **132:** 5411–5424.

Daish, T. J., K. Mills and S. Kumar, 2004 Drosophila caspase DRONC is required for specific developmental cell death pathways and stress-induced apoptosis. Dev. Cell **7:** 909–915.

Danilova, N., K. M. Sakamoto and S. Lin, 2008 Ribosomal protein S19 deficiency in zebrafish leads to developmental abnormalities and defective erythropoiesis through activation of p53 protein family. Blood **112:** 5228–5237.

de Vries, H. I., L. Uyetake, W. Lemstra, J. F. Brunsting, T. T. Su *et al.*, 2005 Grp/DChk1 is required for G2-M checkpoint activa-

tion in Drosophila S2 cells, whereas Dmnk/DChk2 is dispensable. J. Cell Sci. **118:** 1833–1842.

Draptchinskaia, N., P. Gustavsson, B. Andersson, M. Pettersson, T. N. Willig *et al.*, 1999 The gene encoding ribosomal protein S19 is mutated in Diamond-Blackfan anaemia. Nat. Genet. **21:** 169–175.

Engels, W. R., W. K. Benz, C. R. Preston, P. L. Graham, R. W. Phillis *et al.*, 1987 Somatic effects of *P* element activity in *Drosophila melanogaster*: pupal lethality. Genetics **117:** 745–757.

Flores, E. R., K. Y. Tsai, D. Crowley, S. Sengupta, A. Yang *et al.*, 2002 p63 and p73 are required for p53-dependent apoptosis in response to DNA damage. Nature **416:** 560–564.

Flygare, J., and S. Karlsson, 2007 Diamond-Blackfan anemia: erythropoiesis lost in translation. Blood **109:** 3152–3154.

Fogarty, P., S. D. Campbell, R. Abu-Shumays, B. S. Phalle, K. R. Yu *et al.*, 1997 The Drosophila grapes gene is related to checkpoint gene chk1/rad27 and is required for late syncytial division fidelity. Curr. Biol. **7:** 418–426.

Gatti, M., C. Tanzarella and G. Olivieri, 1974 Analysis of the chromosome aberrations induced by x-rays in somatic cells of Drosophila melanogaster. Genetics **77:** 701–719.

Gazda, H. T., and C. A. Sieff, 2006 Recent insights into the pathogenesis of Diamond-Blackfan anaemia. Br. J. Haematol. **135:** 149–157.

Gazda, H. T., A. T. Kho, D. Sanoudou, J. M. Zaucha, I. S. Kohane *et al.*, 2006 Defective ribosomal protein gene expression alters transcription, translation, apoptosis, and oncogenic pathways in Diamond-Blackfan anemia. Stem Cells **24:** 2034–2044.

Goyal, G., B. Fell, A. Sarin, R. J. Youle and V. Sriram, 2007 Role of mitochondrial remodeling in programmed cell death in Drosophila melanogaster. Dev. Cell **12:** 807–816.

Hari, K. L., A. Santerre, J. J. Sekelsky, K. S. McKim, J. B. Boyd *et al.*, 1995 The mei-41 gene of D. melanogaster is a structural and functional homolog of the human ataxia telangiectasia gene. Cell **82:** 815–821.

Harper, J. W., and S. J. Elledge, 2007 The DNA damage response: ten years after. Mol. Cell **28:** 739–745.

Helton, E. S., and X. Chen, 2007 p53 modulation of the DNA damage response. J. Cell Biochem. **100:** 883–896.

Holley, C. L., M. R. Olson, D. A. Colon-Ramos and S. Kornbluth, 2002 Reaper eliminates IAP proteins through stimulated IAP degradation and generalized translational inhibition. Nat. Cell Biol. **4:** 439–444.

Irwin, M. S., K. Kondo, M. C. Marin, L. S. Cheng, W. C. Hahn *et al.*, 2003 Chemosensitivity linked to p73 function. Cancer Cell **3:** 403–410.

Jaklevic, B. R., and T. T. Su, 2004 Relative contribution of DNA repair, cell cycle checkpoints, and cell death to survival after DNA damage in Drosophila larvae. Curr. Biol. **14:** 23–32.

Jassim, O. W., J. L. Fink and R. L. Cagan, 2003 Dmp53 protects the Drosophila retina during a developmentally regulated DNA damage response. EMBO J. **22:** 5622–5632.

Johnson-Schlitz, D. M., C. Flores and W. R. Engels, 2007 Multiple-pathway analysis of double-strand break repair mutations in Drosophila. PLoS Genet. **3:** e50.

Kanda, H., and M. Miura, 2004 Regulatory roles of JNK in programmed cell death. J. Biochem. **136:** 1–6.

Kondo, S., N. Senoo-Matsuda, Y. Hiromi and M. Miura, 2006 DRONC coordinates cell death and compensatory proliferation. Mol. Cell. Biol. **26:** 7258–7268.

Kusch, T., L. Florens, W. H. Macdonald, S. K. Swanson, R. L. Glaser *et al.*, 2004 Acetylation by Tip60 is required for selective histone variant exchange at DNA lesions. Science **306:** 2084–2087.

Lannan, E., R. Vandergaast and P. D. Friesen, 2007 Baculovirus caspase inhibitors P49 and P35 block virus-induced apoptosis downstream of effector caspase DrICE activation in Drosophila melanogaster cells. J. Virol. **81:** 9319–9330.

Lee, J. H., E. Lee, J. Park, E. Kim, J. Kim *et al.*, 2003 In vivo p53 function is indispensable for DNA damage-induced apoptotic signaling in Drosophila. FEBS Lett. **550:** 5–10.

Lindsley, D. L., L. Sandler, B. S. Baker, A. T. Carpenter, R. E. Denell *et al.*, 1972 Segmental aneuploidy and the genetic gross structure of the Drosophila genome. Genetics **71:** 157–184.

Luo, X., O. Puig, J. Hyun, D. Bohmann and H. Jasper, 2007 Foxo and Fos regulate the decision between cell death and survival in response to UV irradiation. EMBO J. **26:** 380–390.

Martin, F. A., A. Perez-Garijo, E. Moreno and G. Morata, 2004 The brinker gradient controls wing growth in Drosophila. Development **131:** 4921–4930.

Martin-Blanco, E., A. Gampel, J. Ring, K. Virdee, N. Kirov *et al.*, 1998 Puckered encodes a phosphatase that mediates a feedback loop regulating JNK activity during dorsal closure in Drosophila. Genes Dev. **12:** 557–570.

Marygold, S. J., J. Roote, G. Reuter, A. Lambertsson, M. Ashburner *et al.*, 2007 The ribosomal protein genes and Minute loci of Drosophila melanogaster. Genome Biol. **8:** R216.

McEwen, D. G., and M. Peifer, 2005 Puckered, a Drosophila MAPK phosphatase, ensures cell viability by antagonizing JNK-induced apoptosis. Development **132:** 3935–3946.

Moon, N. S., L. Di Stefano, E. J. Morris, R. Patel, K. White *et al.*, 2008 E2F and p53 induce apoptosis independently during Drosophila development but intersect in the context of DNA damage. PLoS Genet. **4:** e1000153.

Moreno, E., K. Basler and G. Morata, 2002 Cells compete for decapentaplegic survival factor to prevent apoptosis in Drosophila wing development. Nature **416:** 755–759.

Murray-Zmijewski, F., D. P. Lane and J. C. Bourdon, 2006 p53/p63/p73 isoforms: an orchestra of isoforms to harmonise cell differentiation and response to stress. Cell Death Differ. **13:** 962–972.

Oikemus, S. R., N. McGinnis, J. Queiroz-Machado, H. Tukachinsky, S. Takada *et al.*, 2004 Drosophila atm/telomere fusion is required for telomeric localization of HP1 and telomere position effect. Genes Dev. **18:** 1850–1861.

Oikemus, S. R., J. Queiroz-Machado, K. Lai, N. McGinnis, C. Sunkel *et al.*, 2006 Epigenetic telomere protection by Drosophila DNA damage response pathways. PLoS Genet. **2:** e71.

Ollmann, M., L. M. Young, C. J. Di Como, F. Karim, M. Belvin *et al.*, 2000 Drosophila p53 is a structural and functional homolog of the tumor suppressor p53. Cell **101:** 91–101.

Olson, M. R., C. L. Holley, S. J. Yoo, J. R. Huh, B. A. Hay *et al.*, 2003 Reaper is regulated by IAP-mediated ubiquitination. J. Biol. Chem. **278:** 4028–4034.

Ozaki, T., and A. Nakagawara, 2005 p73, a sophisticated p53 family member in the cancer world. Cancer Sci. **96:** 729–737.

Panic, L., S. Tamarut, M. Sticker-Jantscheff, M. Barkic, D. Solter *et al.*, 2006 Ribosomal protein S6 gene haploinsufficiency is associated with activation of a p53-dependent checkpoint during gastrulation. Mol. Cell. Biol. **26:** 8880–8891.

Peters, M., C. DeLuca, A. Hirao, V. Stambolic, J. Potter *et al.*, 2002 Chk2 regulates irradiation-induced, p53-mediated apoptosis in Drosophila. Proc. Natl. Acad. Sci. USA **99:** 11305–11310.

Reinhardt, H. C., A. S. Aslanian, J. A. Lees and M. B. Yaffe, 2007 p53-deficient cells rely on ATM- and ATR-mediated checkpoint signaling through the p38MAPK/MK2 pathway for survival after DNA damage. Cancer Cell **11:** 175–189.

Riley, T., E. Sontag, P. Chen and A. Levine, 2008 Transcriptional control of human p53-regulated genes. Nat. Rev. Mol. Cell. Biol. **9:** 402–412.

Roos, W. P., and B. Kaina, 2006 DNA damage-induced cell death by apoptosis. Trends Mol. Med. **12:** 440–450.

Ryoo, H. D., T. Gorenc and H. Steller, 2004 Apoptotic cells can induce compensatory cell proliferation through the JNK and the Wingless signaling pathways. Dev. Cell **7:** 491–501.

Sancar, A., L. A. Lindsey-Boltz, K. Unsal-Kacmaz and S. Linn, 2004 Molecular mechanisms of mammalian DNA repair and the DNA damage checkpoints. Annu. Rev. Biochem. **73:** 39–85.

Senoo, M., J. P. Manis, F. W. Alt and F. McKeon, 2004 p63 and p73 are not required for the development and p53-dependent apoptosis of T cells. Cancer Cell **6:** 85–89.

Sidi, S., T. Sanda, R. D. Kennedy, A. T. Hagen, C. A. Jette *et al.*, 2008 Chk1 suppresses a caspase-2 apoptotic response to DNA damage that bypasses p53, Bcl-2, and caspase-3. Cell **133:** 864–877.

Silva, E., S. Tiong, M. Pedersen, E. Homola, A. Royou *et al.*, 2004 ATM is required for telomere maintenance and chromosome stability during Drosophila development. Curr. Biol. **14:** 1341–1347.

Sogame, N., M. Kim and J. M. Abrams, 2003 Drosophila p53 preserves genomic stability by regulating cell death. Proc. Natl. Acad. Sci. USA **100:** 4696–4701.

Song, Y. H., G. Mirey, M. Betson, D. A. Haber and J. Settleman, 2004 The Drosophila ATM ortholog, dATM, mediates the response to ionizing radiation and to spontaneous DNA damage during development. Curr. Biol. **14:** 1354–1359.

Steller, H., 2008 Regulation of apoptosis in Drosophila. Cell Death Differ. **15:** 1132–1138.

Titen, S. W., and K. G. Golic, 2008 Telomere loss provokes multiple pathways to apoptosis and produces genomic instability in *Drosophila melanogaster*. Genetics **180:** 1821–1832.

Tyler, D. M., W. Li, N. Zhuo, B. Pellock and N. E. Baker, 2007 Genes affecting cell competition in Drosophila. Genetics **175:** 643–657.

Umemori, M., O. Habara, T. Iwata, K. Maeda, K. Nishinoue *et al.*, 2009 RNAi-mediated knockdown showing impaired cell survival in Drosophila wing imaginal disc. Gene Regul. Syst. Biol. **3:** 11–20.

Urist, M., T. Tanaka, M. V. Poyurovsky and C. Prives, 2004 p73 induction after DNA damage is regulated by checkpoint kinases Chk1 and Chk2. Genes Dev. **18:** 3041–3054.

Waldhuber, M., K. Emoto and C. Petritsch, 2005 The Drosophila caspase DRONC is required for metamorphosis and cell death in response to irradiation and developmental signals. Mech. Dev. **122:** 914–927.

Wichmann, A., B. Jaklevic and T. T. Su, 2006 Ionizing radiation induces caspase-dependent but Chk2- and p53-independent cell death in *Drosophila melanogaster*. Proc. Natl. Acad. Sci. USA **103:** 9952–9957.

Xu, J., S. Xin and W. Du, 2001 Drosophila Chk2 is required for DNA damage-mediated cell cycle arrest and apoptosis. FEBS Lett. **508:** 394–398.

Xu, D., Y. Wang, R. Willecke, Z. Chen, T. Ding *et al.*, 2006 The effector caspases drICE and dcp-1 have partially overlapping functions in the apoptotic pathway in Drosophila. Cell Death Differ. **13:** 1697–1706.

Xue, D., and H. R. Horvitz, 1995 Inhibition of the Caenorhabditis elegans cell-death protease CED-3 by a CED-3 cleavage site in baculovirus p35 protein. Nature **377:** 248–251.

Yu, S. Y., S. J. Yoo, L. Yang, C. Zapata, A. Srinivasan *et al.*, 2002 A pathway of signals regulating effector and initiator caspases in the developing Drosophila eye. Development **129:** 3269–3278.

Yuan, Z. M., H. Shioya, T. Ishiko, X. Sun, J. Gu *et al.*, 1999 p73 is regulated by tyrosine kinase c-Abl in the apoptotic response to DNA damage. Nature **399:** 814–817.

Communicating editor: E. Alani

GENETICS

Supporting Information
http://www.genetics.org/cgi/content/full/genetics.109.102327/DC1

p53-Independent Apoptosis Limits DNA Damage-Induced Aneuploidy

Laura M. McNamee and Michael H. Brodsky

DOI: 10.1534/genetics.109.102327

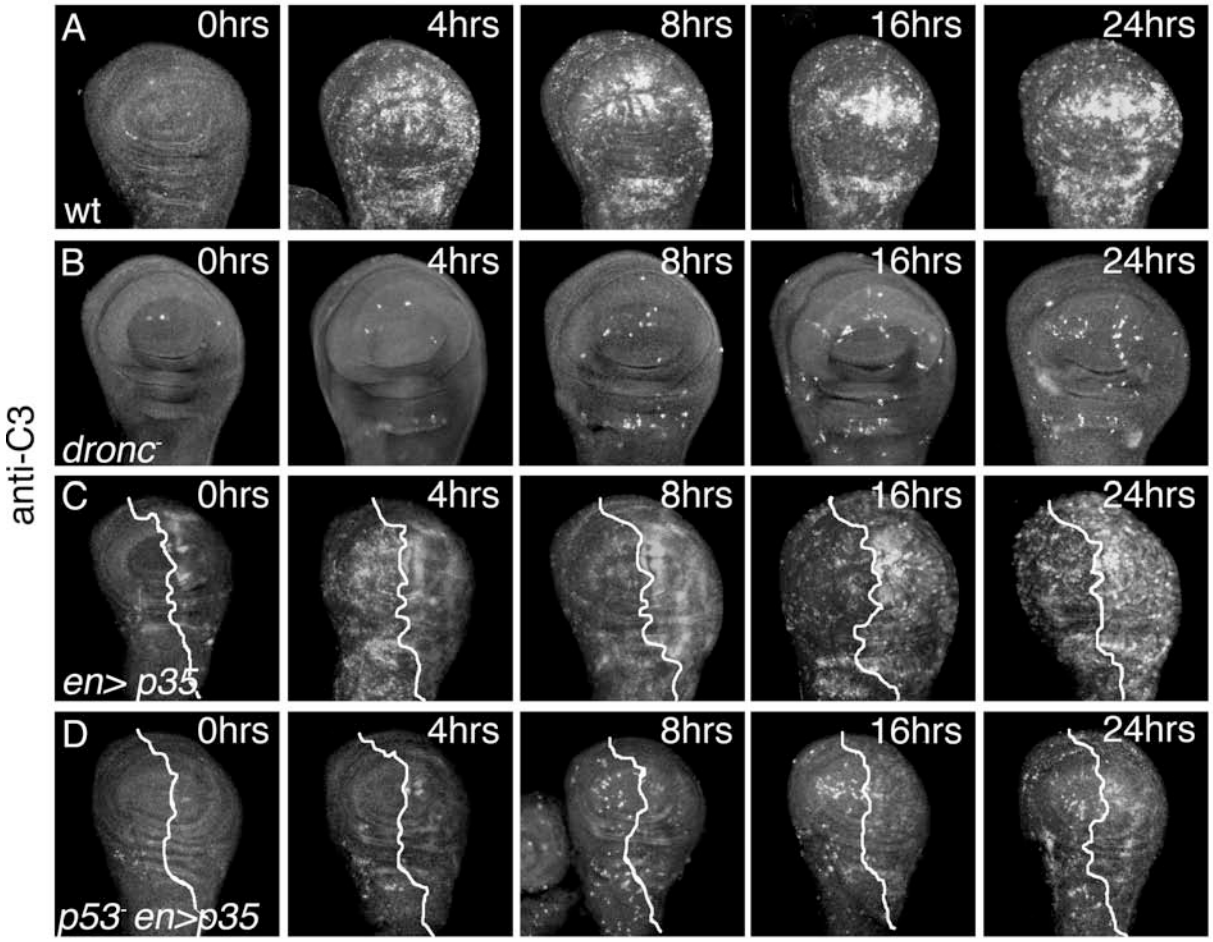

FIGURE S1.—Basal and apical caspases regulate p53-independent induction of the apoptotic marker anti-C3. In all panels, anti-C3 (cleaved caspase 3) staining is used to detect apoptosis. (A) In wild type discs, p53-dependent apoptosis is observed 4 hours following IR. (B) Anti-C3 staining is not induced in wing discs mutant for the apical caspase Dronc. (C and D) The baculovirus protein p35, which blocks the activity of effector caspases following cleavage by apical caspases, is expressed under control of the posterior-specific driver *en*Gal4. In an otherwise wild type disc, the pattern of anti-C3 staining is initially altered following IR treatment and continues to accumulate over time. In a *p53* mutant wing disc, more diffuse anti-C3 staining accumulates by 24 hours following IR treatment.

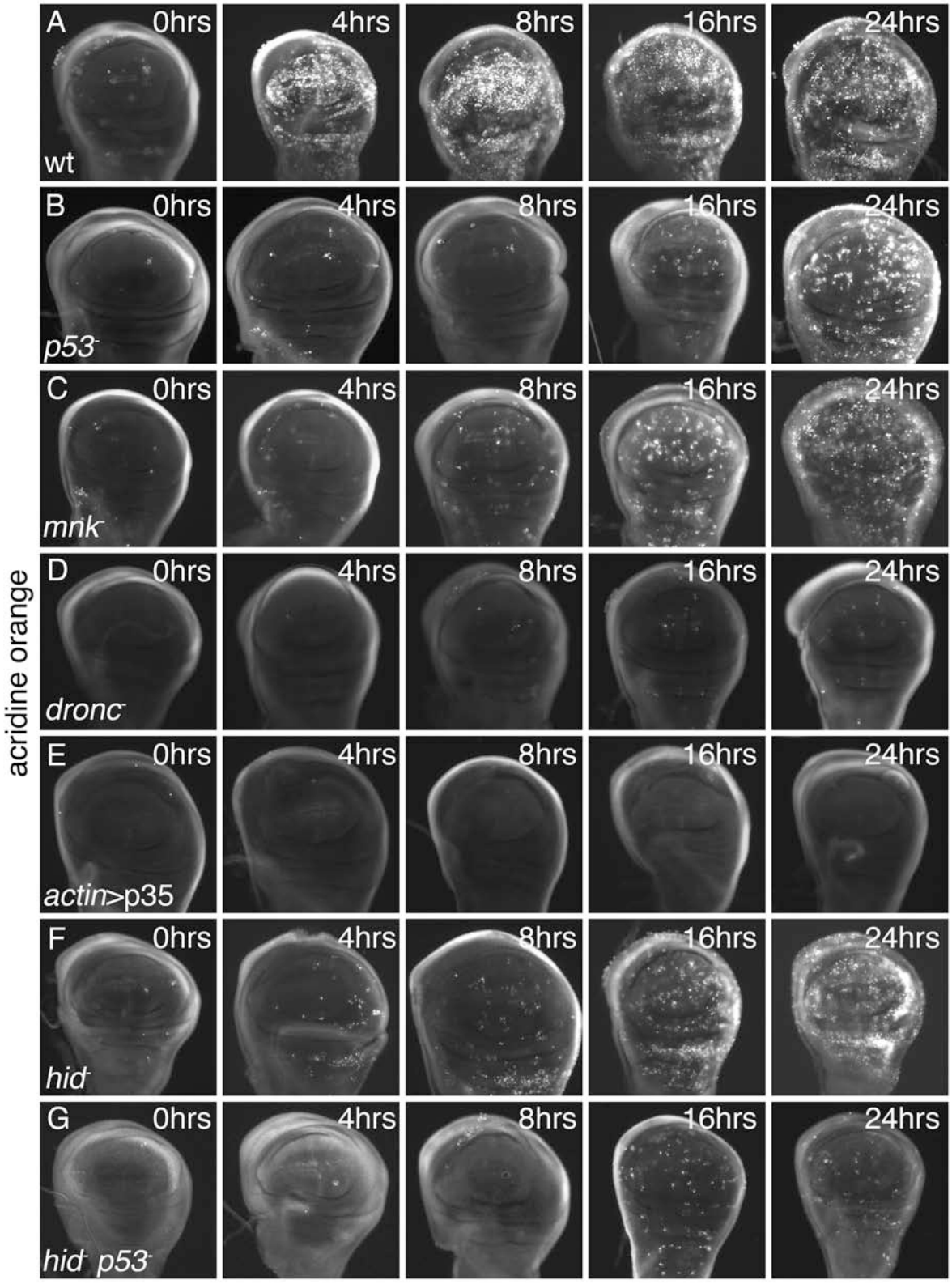

FIGURE S2.—Basal caspases, apical caspases and HID regulate p53-independent induction of the cell death marker acridine orange. (A) p53-dependent apoptosis is observed four hours following IR. (B and C) p53- and MNK-independent apoptosis begins between 8 and 16 hours following IR. (D and E) Acridine orange staining is not induced in wings discs lacking the apical caspase Dronc or expressing the baculovirus protein p35 (under control of the ubiquitous actinGal4 driver), which inhibits the activity of the effector caspases Dcp-1 and Drice. (F and G) The pro-apoptotic gene *hid* contributes to both p53-dependent apoptosis at early time points and to p53-independent apoptosis at late time points.

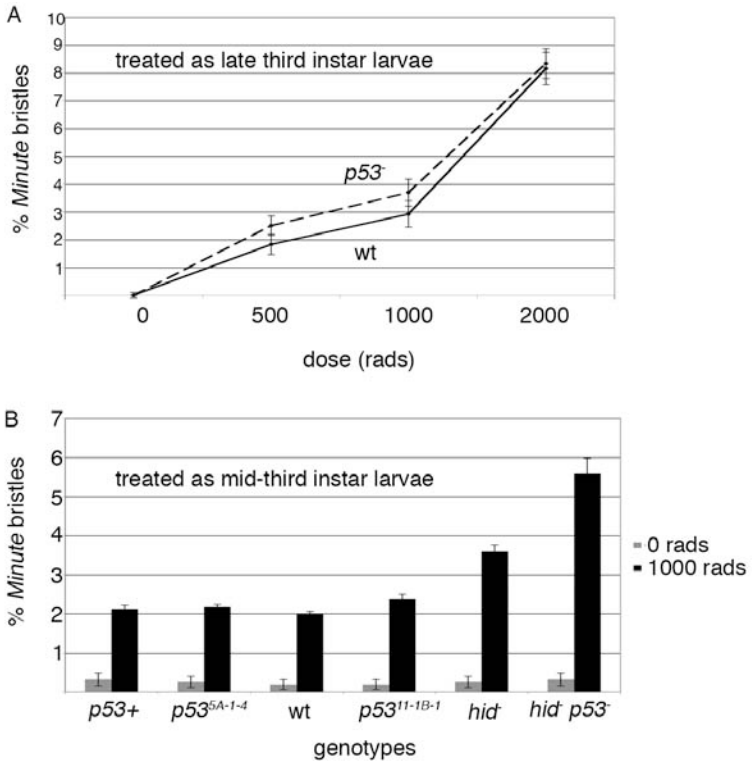

FIGURE S3.—p53-dependent apoptosis does not reduce the number of *Minute* cells following IR. (A) Wandering third instar *p53*- or wild type animals were treated with 500, 1000, and 2000 rads of irradiation or mock treated. This is the same stage used in a previous publication (LEE *et al.* 2003). Twenty-five animals were scored for each genotype in three independent experiments. No significant difference in *Minute* bristles is observed between wt or *p53*- at any dose (n = 3, *P*-value > 0.05). Error bars indicate standard error of the mean. (B) An additional wild type chromosome (*p53*+) and *p53*- allele (*p53*$^{5A\text{-}1\text{-}4}$) were scored for *Minute* bristles after treatment with 1000 rads of irradiation during second to early third instar larvae. The additional wild type allele is an isogenic control for *p53*$^{11\text{-}1B\text{-}1}$ isolated in parallel to the original mutation. Note that the remaining data overlaps data presented for 1000 rads in Figure 6. Sixty animals were scored for each genotype in three independent experiments. There was no significant difference in *Minute* bristles following IR in these alleles compared to wild type (n = 3, *P*-value > 0.05). Error bars indicate standard error of the mean.

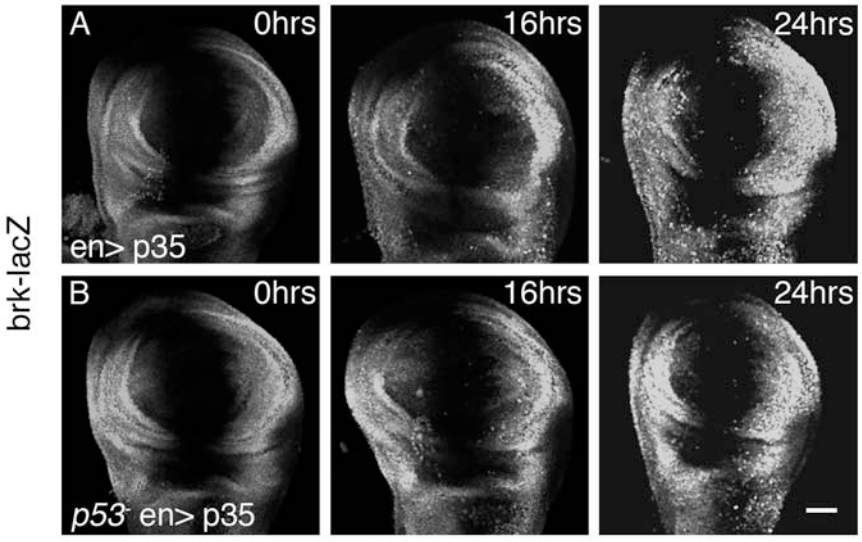

FIGURE S4.—*brk* is ectopically expressed following irradiation of discs with wild type p53 function. (A) Ectopic expression of *brk* following IR is observed following irradiation of discs with wild type *p53* function that express p35; this result indicates that the absence of p53 is not required for this response. (B) Similar levels of ectopic *brk* following IR are also observed in *p53* mutant wing discs expressing p35. Scale bar = 50μm.

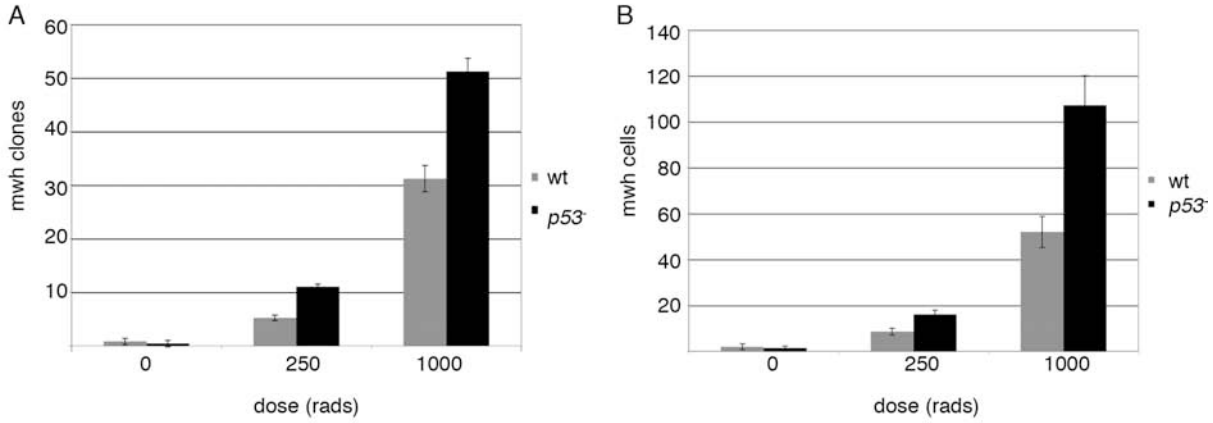

FIGURE S5.—p53-dependent apoptosis limits the accumulation of *mwh*$^{-/-}$ cells following IR. Wandering third instar larvae heterozygous for a mutation in the *mwh* locus were treated with 0, 250, or 1000 rads. The average number of *mwh*$^{-/-}$ clones (A) or cells (B) per wing was calculated to determine rates of loss of heterozygosity (LOH) as previously described (BAKER *et al.* 1978; BRODSKY *et al.* 2000b). *p53* mutant wings had more *mwh* mutant clones and mutant cells than wild type at both doses (n = 5, *P*-value < 0.05), confirming a previously published conclusion (SOGAME *et al.* 2003). Error bars indicate standard error of the mean.